

Written Comprehensive Exam:

Improved Trial Wave Function for Quantum Monte Carlo Calculations of Nuclear Systems

Cody L. Petrie
Advisor: Kevin Schmidt

March 15, 2017

Abstract

We have done Auxiliary Field Diffusion Monte Carlo calculations to determine the energy of ^4He and ^{16}O and the energy per nucleon of symmetric nuclear matter (SNM) with 28 particles in a periodic box with density $\rho = 0.16\text{fm}^{-3}$. These calculations have been done with two new types of correlations in the trial wave function that include quadratic terms in the expansion of the correlation term. These results have been compared to previous results done with linear correlations.

1 Motivation

Understanding the interactions between nucleons has been a lengthy and difficult task to pursue for science. However, a thorough understanding of these interactions would give us great insight into the structure of nuclei, the r-process by which nucleosynthesis occurs in supernovae, as well as the formation of neutron stars [1–5]. Both of these areas of research are difficult to probe experimentally and would benefit greatly from good theoretical predictions to guide experiments in useful and exciting directions.

Despite the difficulty, science has been making continuous steps towards understanding these interactions. In 1935 Hideki Yukawa proposed the idea that this interaction, called the strong force, was governed by quanta or exchange particles [6], which were later called pions [7]. He proposed what is now called the Yukawa potential, which is still used in modified form in many nuclear models today, to describe these interactions. The range of the force proposed by Yukawa was inversely proportional to the mass of the pion, and the strength of the force was based only on the distance separating the particles. Today we often use potentials that depend on the separation distance between the particles, but also their relative spins and isospins. These interactions can be quite complicated, making a true understanding of the strong force difficult to achieve.

Currently Quantum Chromodynamics (QCD) is believed to be the correct underlying theory to describe the strong force [8]. However, this theory currently cannot be solved for nuclear particles, although some progress is being made. For example, calculations of

n-n scattering have been done but they return pion masses that are too large, $m_\pi \sim 450$ MeV [9]. Instead approximate methods often based on effective field theories are used. The development of low energy effective field theories would provide useful insights into the nuclear force, even if we had low energy solutions to QCD.

A set of approximate methods called basis set methods are often used to solve for properties of nuclei. Some of these methods are the no core shell model [10,11], the coupled-cluster method [12], and the self-consistent Green's function method [13,14]. For these methods the wave function of the nuclear system is written in terms of a truncated basis, often a harmonic oscillator basis. The momentum cutoff of the basis needs to be higher than the important momenta of the interaction that is being used, in order to do calculations in momentum space. This means however that calculations with sharp potentials (like local hard wall potentials) are difficult to do with basis set methods. They do employ techniques such as Similarity Renormalization Group [15] to soften these types of interaction. This allows them to decrease the number of basis functions used. One of the advantages of basis set methods is that they can use local and non-local, i.e. velocity dependent, potentials. The Quantum Monte Carlo [16] methods, which we are using in this work, complement these basis set methods. Although they are currently limited to mostly local potentials¹ [17], they can converge for a wide variety of local Hamiltonians. Also, Quantum Monte Carlo methods do not have the momentum cutoff limits or the poor scaling with basis set size of the basis set methods.

Using these approximate methods to study nuclear systems will allow us to better understand the interactions between nuclei and ultimately will advance our understanding of many important processes in the universe.

2 Methods

Many of the methods that are used to work on nuclear many-body problems are approximate. The method that we will be using and describing in the following sections is the Quantum Monte Carlo method [16].

Many methods that use the variational principle start with a trial wave function similar to the one used in Hartree-Fock calculations [18], sometimes with Jastrow-like correlations [19]. However, to get an upper bound on energies they usually have to solve some sort of differential equation or multi-dimensional integrals. Especially if complicated spin-isospin dependent correlations are applied to the trial wave function, these integrals can be quite difficult to solve. Quantum Monte Carlo calculations use statistical sampling to get solutions with controlled statistical errors to large integrals that would otherwise be intractable. For a good review of Quantum Monte Carlo methods we refer the reader to [16,20–22]. Here we will describe the methods that we have used in this research, those being Variational, Diffusion, and Auxiliary Field Diffusion Monte Carlo methods. Before describing those methods we are going to introduce the ideas of Monte Carlo integration and the Metropolis algorithm. Both of these tools will be used in the various Quantum Monte Carlo techniques.

¹Currently, interactions that are linear in the momentum can be used. Higher order terms are treated perturbatively.

2.1 Monte Carlo Integration

We will illustrate Monte Carlo Integration by imagining that we want to integrate the function $g(\mathbf{R})$ where $\mathbf{R} = \mathbf{r}_1, \mathbf{r}_2, \dots, \mathbf{r}_n$, so

$$I = \int g(\mathbf{R}) d\mathbf{R}. \quad (1)$$

We can rewrite this integral in terms of a probability density called an importance function $P(\mathbf{R})$, and $f(\mathbf{R}) = g(\mathbf{R})/P(\mathbf{R})$.

$$I = \int f(\mathbf{R}) P(\mathbf{R}) d\mathbf{R} \equiv \langle f \rangle \quad (2)$$

This integral is the expectation value of $f(\mathbf{R})$ as long as the \mathbf{R} 's are distributed according to $P(\mathbf{R})$. Thus we can find the integral by finding the expectation value. One way to do that would be to take an infinite number of sample configurations from the importance function and evaluate the average of $f(\mathbf{R})$ given that infinite set of samples,

$$I = \lim_{N \rightarrow \infty} \frac{1}{N} \sum_{n=1}^N f(\mathbf{R}_n). \quad (3)$$

Since we cannot take an infinite number of samples, we can approximate the integral by taking a large number of samples, and finding an approximate expectation value from that finite set.

$$I \approx \frac{1}{N} \sum_{n=1}^N f(\mathbf{R}_n). \quad (4)$$

The statistical uncertainty for the estimate of the integral is given in the typical way.

$$\sigma_I = \sqrt{\frac{\langle f^2 \rangle - \langle f \rangle^2}{N}} \approx \sqrt{\frac{\left(\frac{1}{N} \sum_{n=1}^N f^2(\mathbf{R}_n) \right) - \left(\frac{1}{N} \sum_{n=1}^N f(\mathbf{R}_n) \right)^2}{N-1}} \quad (5)$$

Notice that the scaling is independent of the dimension, and thus this method is useful especially when the dimensions of the integration become large. In many-body quantum mechanics the dimension of the integrals can be quite large, including several dimensions for each particle in the calculation. Monte Carlo integration only needs to sample each of these dimensions, decreasing the work required by a substantial amount for large dimensional integrals.

2.2 Metropolis Algorithm

To do Monte Carlo integration random variables \mathbf{R}_n need to be sampled from the importance function, $P(\mathbf{R})$. If the inverse cumulative distribution function of the probability distribution exists, $F^{-1}(\mathbf{R})$, this is straightforward to do. In the one dimensional case a random variables x could be sampled by drawing a random variable u from a uniform distribution from 0

to 1, which is then used as an argument of the inverse cumulative distribution function, $x = F^{-1}(u)$. This works assuming the inverse of the cumulative distribution function can be found. But let's say that we cannot find the inverse. This is where the Metropolis algorithm comes in, allowing us to get random samples from $P(x)$ without knowing $F^{-1}(u)$. The Metropolis algorithm is a Markov Chain method that uses only the previous point to determine where the next move will be, i.e. the step does not depend on history other than the previous step. These are the steps to the algorithm.

1. Start at a random position, \mathbf{R} .
2. Propose a move to a new position \mathbf{R}' , pulled from a distribution $T(\mathbf{R}'|\mathbf{R})$. T could be, for example, a Gaussian centered on the current position, but could be optimized for efficiency.
3. The probability of accepting the move is given by enforcing a detailed balance condition².

$$A(\mathbf{R}'|\mathbf{R}) = \min \left(1, \frac{P(\mathbf{R}')T(\mathbf{R}|\mathbf{R}')}{P(\mathbf{R})T(\mathbf{R}'|\mathbf{R})} \right) \quad (6)$$

4. A random number, u , is generated from a uniform distribution between 0 and 1, and the move is accepted if $A \geq u$.

2.3 Variational Monte Carlo

Variational Monte Carlo (VMC) starts with a trial wave function, ψ_T , that should have some non-zero overlap with the actual ground-state wave function, and a Hamiltonian, H . The expectation value of the Hamiltonian in the trial state gives what is called the variational energy. By the variational principle this energy is guaranteed to be an upper bound on the true ground-state wave function.

$$E_V = \frac{\int \psi_T^*(\mathbf{R}) H \psi_T(\mathbf{R}) d\mathbf{R}}{\int \psi_T^*(\mathbf{R}) \psi_T(\mathbf{R}) d\mathbf{R}} \geq E_0 \quad (7)$$

We want to do this integral using Monte Carlo integration and so we need it to look like Eq. 2. One way to get it into this form is to multiply the top integrand by $\psi_T(\mathbf{R})\psi_T^{-1}(\mathbf{R})$ which gives

$$E_V = \int P(\mathbf{R}) E_L(\mathbf{R}) d\mathbf{R}, \quad (8)$$

where

$$P(\mathbf{R}) = |\Psi_T(\mathbf{R})|^2 / \int |\Psi_T(\mathbf{R})|^2 d\mathbf{R}, \quad (9)$$

$$E_L(\mathbf{R}) = \frac{\Psi_T^*(\mathbf{R}) H \Psi_T(\mathbf{R})}{\Psi_T^*(\mathbf{R}) \Psi_T(\mathbf{R})}, \quad (10)$$

²There are two conditions that need to be met to guarantee that this algorithm converges to the desired distribution. First, the transitions must be able to get from any allowed state to another in a finite number of steps. Second, the algorithm cannot include cycles between the same states. This second condition is guaranteed if there is a probability to reject transitions.

are the importance function and local energy respectively.

Now using the metropolis algorithm we can draw a set of random configurations, $\{\mathbf{R}_n : n = 1, N\}$ from the probability distribution $P(\mathbf{R})$ and use those to sample the local energy. These random configurations are called walkers and contain the positions, and sometimes spins and isospins, of each particle. The variational energy and corresponding statistical error are then given by,

$$E_V \approx \frac{1}{N} \sum_{n=1}^N E_L(\mathbf{R}_n), \quad (11)$$

$$\sigma_{E_V} = \sqrt{\frac{\langle E_L^2 \rangle - \langle E_L \rangle^2}{N}} \approx \sqrt{\frac{\left(\frac{1}{N} \sum_{n=1}^N E_L^2(\mathbf{R}_n) \right) - \left(\frac{1}{N} \sum_{n=1}^N E_L(\mathbf{R}_n) \right)^2}{N-1}} \quad (12)$$

At this point certain parameters in Ψ_T can be varied until a minimum in the energy is found. A minimum in the energy will be produced when $\Psi_T \rightarrow \Psi_0$. It is important to note however that the trial wave functions that we often use are not exactly the ground-state wave functions and so the energies that we produce are only the minimum energy for that specific trial wave function. That is why it is important to start with the best trial wave function possible.

2.4 Diffusion Monte Carlo

Diffusion Monte Carlo (DMC) solves for the ground-state by letting the walkers diffuse in imaginary time. Starting with the Schrödinger equation

$$H\Psi = i\hbar \frac{\partial \Psi}{\partial t}. \quad (13)$$

Now we substitute time for imaginary time using $\tau = it/\hbar$ and notice that this looks similar to the diffusion equation.

$$H\Psi = -\frac{\partial \Psi}{\partial \tau} \quad (14)$$

By separating variables we can write the solution as eigenfunctions in spatial coordinates times an exponential in imaginary time where we have shifted the energies by a parameter, E_0 that we can use to control the normalization, $V \rightarrow V - E_0$ and $E_n \rightarrow E_n - E_0$.

$$\Psi(\mathbf{R}, \tau) = \sum_{n=0}^{\infty} c_n \phi_n(\mathbf{R}) e^{-\tau(E_n - E_0)} \quad (15)$$

Then one of the key parts of DMC is that as you let $\tau \rightarrow \infty$ all of the states higher than the ground-state fall off because the difference, $E_n - E_0$, is non-zero and the exponential tends to zero because of the infinite τ . This leaves only the ground-state,

$$\lim_{\tau \rightarrow \infty} \Psi(\mathbf{R}, \tau) = c_0 \phi_0(\mathbf{R}). \quad (16)$$

Since we cannot generally compute this limit, $\lim_{\tau \rightarrow \infty} \Psi(\mathbf{R}, \tau) = \lim_{\tau \rightarrow \infty} e^{-(H-E_0)\tau} \Psi(\mathbf{R})$, directly we split the propagation into small steps in imaginary time. To do this, insert a complete set of states into the propagated wave function.

$$\langle \mathbf{R}' | \Psi_T(\tau) \rangle = \int d\mathbf{R} \langle \mathbf{R}' | e^{-(H-E_0)\tau} | \mathbf{R} \rangle \langle \mathbf{R} | \Psi_T(0) \rangle \quad (17)$$

Now you can break τ up into N smaller time steps $\Delta\tau = \tau/N$ and insert a complete set of states between each finite time propagator,

$$\langle \mathbf{R}_N | \Psi_T(\tau) \rangle = \int d\mathbf{R}_1 \dots d\mathbf{R}_N \left[\prod_{i=1}^N \langle \mathbf{R}_i | e^{-(H-E_0)\Delta\tau} | \mathbf{R}_{i-1} \rangle \right] \langle \mathbf{R}_0 | \Psi_t(0) \rangle \quad (18)$$

$$= \int d\mathbf{R}_1 \dots d\mathbf{R}_N \left[\prod_{i=1}^N G(\mathbf{R}_i, \mathbf{R}_{i-1}, \Delta\tau) \right] \langle \mathbf{R}_0 | \Psi_t(0) \rangle, \quad (19)$$

where $\mathbf{R}_N = \mathbf{R}'$, $\mathbf{R}_0 = \mathbf{R}$ and $G(\mathbf{R}', \mathbf{R}, \tau) = \langle \mathbf{R}' | e^{-(H-E_0)\tau} | \mathbf{R} \rangle$, is often called the Green's function or the propagator. We cannot calculate the Green's function directly but if the kinetic and potential terms are broken up each piece can be calculated separately.

$$G(\mathbf{R}', \mathbf{R}, \Delta\tau) = \langle \mathbf{R}' | e^{-(V-E_0)\Delta\tau/2} e^{-T\Delta\tau} e^{-(V-E_0)\Delta\tau/2} | \mathbf{R} \rangle \quad (20)$$

$$= e^{(V(\mathbf{R}') + V(\mathbf{R}) - 2E_0)\Delta\tau/2} \langle \mathbf{R}' | e^{-T\Delta\tau} | \mathbf{R} \rangle \quad (21)$$

This break up is equal to the original Green's function up to $\mathcal{O}(\Delta\tau^3)$, and thus the step in imaginary time needs to be kept small. The kinetic term is used to move the walkers and the potential part is used to speed up convergence via a branching algorithm. The kinetic term gives us

$$G_0(\mathbf{R}', \mathbf{R}, \Delta\tau) = \langle \mathbf{R}' | e^{-T\Delta\tau} | \mathbf{R} \rangle, \quad (22)$$

which can be written as a diffusion term

$$G_0(\mathbf{R}', \mathbf{R}, \Delta\tau) = \left(\frac{m}{2\pi\hbar^2\Delta\tau} \right)^{3A/2} e^{-m(\mathbf{R}' - \mathbf{R})^2/2\hbar^2\Delta\tau}, \quad (23)$$

where A is the total number of nucleons. The piece that contains the potential then can be used to give a weight that gets used with the branching algorithm,

$$w(\mathbf{R}') = e^{(V(\mathbf{R}') + V(\mathbf{R}) - 2E_0)\Delta\tau/2}. \quad (24)$$

This sampling can give us large uncertainties and so we often use a function that does a good job describing the system (this can be the trial wave function) to guide the sampling. This function is called an importance function, $\Psi_I(\mathbf{R})$, and thus the method is called importance sampling. The idea is that instead of sampling directly from the Green's function you will sample from

$$G(\mathbf{R}', \mathbf{R}, \Delta\tau) \frac{\langle \mathbf{R} | \Psi_I \rangle}{\langle \mathbf{R}' | \Psi_I \rangle}. \quad (25)$$

It turns out that this greatly improves the variance of the sampling. This is because the importance function will cause the walkers to move towards where the square of the wave function is larger, and thus there is less samples in regions where the wave function is small. The DMC algorithm can generally be written as follows.

1. Generate a set of random walkers. These are typically from a previously done VMC calculation, which has no constraint and provides an upper bound in the energy.
2. For each walker propose a move, $\mathbf{R}' = \mathbf{R} + \chi$, where χ is a vector of random numbers from the shifted Gaussian $\exp\left(\frac{m}{2\hbar^2\Delta\tau}\left(\mathbf{R}' - \mathbf{R} + 2\frac{\nabla\Psi_I(\mathbf{R}')}{\Psi_I(\mathbf{R}')}\right)^2\right)$.
3. For each walker calculate the weight $w(\mathbf{R}') = \exp\left(-\left(\frac{E_L(\mathbf{R}') + E_L(\mathbf{R})}{2} - E_0\right)\Delta\tau\right)$.
4. Do the branching. There are various ways to do this, but the simplest way is to make copies of each walker, where the number of copies for each walker that continues in the calculation is given by $\text{int}(w(\mathbf{R}') + \xi)$, where ξ is a uniform random number from $[0, 1]$. This way walkers with a small weight will more often be removed from the calculation and walkers with high weights will multiply.
5. Calculate and collect the observables and uncertainties needed and increase the imaginary time by $\Delta\tau$.
6. Repeat steps 2 through 5 until the uncertainties are small enough.

This method is described well in Refs. [16] and [22]. Green's function Monte Carlo (GFMC) and auxiliary field diffusion Monte Carlo (AFDMC) use this method to handle the spatial part of the calculation, but they each handle the spin-isospin part differently. Everywhere where the trial wave function is used in GFMC there is an explicit sum over the spin and isospin states. The number of possible spin states given A nucleons is 2^A . The number of isospin states given A nucleons and Z protons can be reduced to $\binom{A}{Z}$ states leaving us with a total of $2^A \binom{A}{Z}$ spin-isospin states. The number of states and the number of operators required for the trial wave function increase exponentially as the number of nucleons increases. To date, the largest nuclei that can be calculated with GFMC is ^{12}C . As a result of this, AFDMC was developed as a way to use Monte Carlo methods to sample the spin states.

2.5 Auxiliary Field Diffusion Monte Carlo

To overcome the exponentially large number of spin-isospin states that have to be summed in GFMC, AFDMC was developed in 1999 [21] to sample these states and, in analogy to moving the position of each walker, rotate the spin and isospin of each walker. To do this we use the basis where an element of the basis contains the three spatial coordinates of each particle and the amplitude for each particle to be in each of the four possible spin-isospin states $|s\rangle = |p\uparrow, p\downarrow, n\uparrow, n\downarrow\rangle$. Now we need to write the spin-isospin dependent part of the propagator in this basis,

$$G_{SD}(R'S', RS, \Delta\tau) = \langle R'S' | e^{-V_{SD}\Delta\tau} | RS \rangle, \quad (26)$$

where V_{SD} does not include the central, non spin-isospin part of the potential. Here the potential can be written as

$$V_{SD} = \sum_{p=2}^M \sum_{i<j} v_p(r_{ij}) \mathcal{O}_{ij}^p, \quad (27)$$

where M is the number of operators (e.g. $M = 6$ for the v_6 potential or $M = 18$ for the Argonne v_{18} two-body potential [23]). In this study we have used the standard v_6 potential which includes the operators $\boldsymbol{\sigma}_i \cdot \boldsymbol{\sigma}_j$, $\boldsymbol{\tau}_i \cdot \boldsymbol{\tau}_j$, $\boldsymbol{\sigma}_i \cdot \boldsymbol{\sigma}_j \boldsymbol{\tau}_i \cdot \boldsymbol{\tau}_j$, S_{ij} and $S_{ij} \boldsymbol{\tau}_i \cdot \boldsymbol{\tau}_j$, where $S_{ij} = 3\boldsymbol{\sigma}_i \cdot \hat{r}_{ij} \boldsymbol{\sigma}_j \cdot \hat{r}_{ij} - \boldsymbol{\sigma}_i \cdot \boldsymbol{\sigma}_j$. Here the σ and τ operators are the Pauli matrices applied to spin and isospin respectively. This potential can be written in the more convenient form

$$V_{SD} = \frac{1}{2} \sum_{i,\alpha,j,\beta} \sigma_{i,\alpha} A_{i,\alpha,j,\beta}^\sigma \sigma_{j,\beta} + \frac{1}{2} \sum_{i,\alpha,j,\beta} \sigma_{i,\alpha} A_{i,\alpha,j,\beta}^{\sigma\tau} \sigma_{j,\beta} \boldsymbol{\tau}_i \cdot \boldsymbol{\tau}_j + \frac{1}{2} \sum_{i,j} A_{i,j}^\tau \boldsymbol{\tau}_i \cdot \boldsymbol{\tau}_j, \quad (28)$$

where we have defined these new A matrices. These matrices are written in terms of the $v_p(r_{ij})$ functions above. For example the simplest matrix is the $A_{i,j}^\tau$ matrix which can be shown to be $A_{i,j}^\tau = v_\tau(r_{ij})$. There is a factor of one half in Eq. 28 because the sums go over all i and j particles instead of pairs for which $i < j$. These matrices are zero when $i = j$ and they are symmetric. We can also write these matrices in terms of their eigenvalues and eigenvectors.

$$\sum_{j,\beta} A_{i,\alpha,j,\beta}^\sigma \psi_{n,j,\beta}^\sigma = \lambda_n^\sigma \psi_{n,i,\alpha}^\sigma \quad (29)$$

$$\sum_{j,\beta} A_{i,\alpha,j,\beta}^{\sigma\tau} \psi_{n,j,\beta}^{\sigma\tau} = \lambda_n^{\sigma\tau} \psi_{n,i,\alpha}^{\sigma\tau} \quad (30)$$

$$\sum_j A_{i,j}^\tau \psi_{n,j}^\tau = \lambda_n^\tau \psi_{n,i}^\tau \quad (31)$$

Written in terms of these eigenvalues and eigenvectors the potential can be written as

$$V_{SD} = \frac{1}{2} \sum_{n=1}^{3A} (O_n^\sigma)^2 \lambda_n^\sigma + \frac{1}{2} \sum_{\alpha=1}^3 \sum_{n=1}^{3A} (O_{n\alpha}^{\sigma\tau})^2 \lambda_n^{\sigma\tau} + \frac{1}{2} \sum_{\alpha=1}^3 \sum_{n=1}^A (O_{n\alpha}^\tau)^2 \lambda_n^\tau, \quad (32)$$

where the operators are given by

$$\begin{aligned} O_n^\sigma &= \sum_{j,\beta} \sigma_{j,\beta} \psi_{n,j,\beta}^\sigma \\ O_{n\alpha}^{\sigma\tau} &= \sum_{j,\beta} \tau_{j,\alpha} \sigma_{j,\beta} \psi_{n,j,\beta}^{\sigma\tau} \\ O_{n\alpha}^\tau &= \sum_j \tau_{j,\alpha} \psi_{n,j}^\tau \end{aligned} \quad (33)$$

These operators in the propagator now have the effect of rotating the spinors, analogous to diffusing the walkers in space. To reduce the order of the operators in the propagator from quadratic to linear we use the Hubbard-Stratanovich transformation.

$$e^{-\frac{1}{2}\lambda O^2} = \frac{1}{\sqrt{2\pi}} \int dx e^{-\frac{x^2}{2} + \sqrt{-\lambda} x O} \quad (34)$$

The variable x is called an auxiliary field. Using the fact that there are $3A$ O_n^σ operators, $9A$ $O_{n\alpha}^{\sigma\tau}$ operators and $3A$ $O_{n\alpha}^\tau$ operators, for a total of $15A$ operators, and by using the

Hubbard-Stratanovich transformation we can write the spin-isospin dependent part of the propagator as

$$\prod_{n=1}^{15A} \frac{1}{\sqrt{2\pi}} \int dx_n e^{-\frac{x_n^2}{2}} e^{\sqrt{-\lambda_n \Delta\tau} x_n O_n}. \quad (35)$$

The spinors are then rotated based on auxiliary fields sampled from the Gaussian with unit variance in Eq. 35.

3 Trial wave function

The trial wave function is used in both the diffusion and branching algorithms and thus it is important that it be close to the ground state wave function of the system. Propagation in imaginary time removes the excited states from the trial wave function and so a larger overlap between the trial wave function and the ground state wave function means quicker convergence in imaginary time. One of the simplest many particle wave functions is an antisymmetrized product of single particle orbitals,

$$\psi_T = \mathcal{A} \prod_{i=1}^A \phi_i(\mathbf{r}_\alpha, s_\alpha) = \frac{1}{A!} \det \phi_i(\mathbf{r}_\alpha, s_\alpha), \quad (36)$$

where \mathcal{A} is an antisymmetrization operator with $\mathcal{A}^2 = \mathcal{A}$. This is often called a Slater determinant. This wave function represents the long range part of the interactions leaving out short range correlations. The simplest short range correlation that can be formed is a spin-isospin independent Jastrow-like correlation only dependent on space,

$$|\psi_T\rangle = \prod_{i<j} f(r_{ij}) |\phi\rangle, \quad (37)$$

where r_{ij} are operators. The most general way to include spin-isospin dependent correlations to a Slater determinant, while maintaining the cluster decomposability of the system, is to use an exponential of the correlation operators.

$$|\psi_T\rangle = \prod_{i<j} f_c(r_{ij}) e^{\sum_p f_p(r_{ij}) \mathcal{O}_{ij}^p} |\phi\rangle \quad (38)$$

The calculation of this trial wave function grows exponentially with particle number, however a symmetrized product of pair operators has nearly the same form at second order, and exactly the same form in the independent pair condition, which we will describe in more detail shortly. The symmetrized product wave function is

$$|\psi_T\rangle = \left[\prod_{i<j} f_c(r_{ij}) \right] \left[\mathcal{S} \prod_{i<j} \left(1 + \sum_p f_p(r_{ij}) \mathcal{O}_{ij}^p \right) \right] |\phi\rangle, \quad (39)$$

where the symmetrization operator \mathcal{S} is

$$\mathcal{S} |R\rangle = \frac{1}{N!} \sum_{|R^p\rangle} |R^p\rangle, \quad (40)$$

and $|R^p\rangle$ are all permutations of the particles coordinates. If you expand this to second order you can write this as

$$|\psi_T\rangle = \left[\prod_{i<j} f_c(r_{ij}) \right] \left[1 + \sum_{i<j} \sum_p f_p(r_{ij}) \mathcal{O}_{ij}^p + \frac{1}{2} \sum_{i<j} \sum_p f_p(r_{ij}) \mathcal{O}_{ij}^p \sum_{\substack{k<l \\ ij \neq kl}} \sum_q f_q(r_{kl}) \mathcal{O}_{kl}^q \right] |\phi\rangle. \quad (41)$$

Notice that the quadratic correlations include all sets of pairs except those with the exact same two particles. The exponential wave function in equation 38 has these terms, with a different factor. Also notice that the quadratic terms are symmetrized by summing over each ij pair and each kl pair and then dividing by two. If instead of taking all possible quadratic pairs, only sets of pairs where the same particle does not appear twice are taken, this is called the independent pair correlation.

$$|\psi_T\rangle = \left[\prod_{i<j} f_c(r_{ij}) \right] \left[1 + \sum_{i<j} \sum_p f_p(r_{ij}) \mathcal{O}_{ij}^p + \sum_{i<j} \sum_p f_p(r_{ij}) \mathcal{O}_{ij}^p \sum_{k<l, \text{ip}} \sum_q f_q(r_{kl}) \mathcal{O}_{kl}^q \right] |\phi\rangle. \quad (42)$$

Here the sum over independent pairs means that no particle is included in both pairs ij and kl , and you do not get the symmetric pair terms, i.e. if you have the set of pairs $ijkl = 1234$, you do not include 3412. This is because the operators in the quadratic terms commute and do not need to be symmetrized. We have done calculations with both of these wave functions and compared the results to calculations done with the linear wave function

$$|\psi_T\rangle = \left[\prod_{i<j} f_c(r_{ij}) \right] \left[1 + \sum_{i<j} \sum_p f_p(r_{ij}) \mathcal{O}_{ij}^p \right] |\phi\rangle. \quad (43)$$

We have added a variational parameter to the quadratic terms, but for most of the results shown here that parameter was set to one, however we do show that the results improve as the variational parameter is optimized.

4 Results

We have calculated energies with all three types of correlations, linear, independent pair, and quadratic, and compared the results. In all cases we have used the v6 potential and the same operators for the correlations. In each case the weights for each operator were determined variationally. Calculations were done for systems, ^4He and ^{16}O and the energies are reported in Table 1 with and without independent pair correlations and compared to the experimental value.

We have also calculated the energy per nucleon of symmetric nuclear matter (SNM) with density $\rho = 0.16\text{fm}^{-3}$ of 28 particles with periodic boundary conditions. The energy per nucleon was -13.92(6) MeV for linear correlations, -14.80(7) MeV for independent pair correlations, and -14.70(11) MeV with the full set of quadratic correlations.

Notice that in the case of ^{16}O and SNM the independent pair and quadratic correlations caused the energies to decrease, while in the case of ^4He the energy went up when independent

Table 1: Energy in MeV for ^4He and ^{16}O as calculated with all three types of correlations compared to experimental energies.

	Linear	IndPair	Quadratic	Expt.
^4He	-27.17(4)	-26.33(3)	-25.35(3)	-28.295
^{16}O	-115.7(9)	-121.5(1.5)	-120.0(1.4)	-127.619

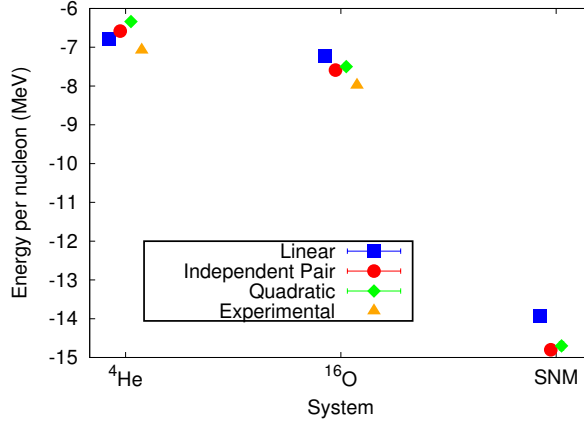


Figure 1: Energy per nucleon for ^4He and ^{16}O as calculated with linear, independent pair and quadratic correlations. Also, the energy per nucleon of symmetric nuclear matter of 28 particles in a periodic box with density $\rho = 0.16\text{fm}^{-3}$. All calculations are compared to their expected values.

pair correlations were added, and even more when the quadratic correlations were added. We expected the energies and uncertainties to decrease a little for each calculation since we were using a more correct wave function. This was true for ^{16}O and SNM, but not for ^4He . The energy for ^4He increased with both new types of correlations. At first we thought that this could be due to the small number of extra terms in the independent pair correlation with only 4 particles, however the quadratic correlations, which have many more terms, also caused the energy to increase. The original linearly correlated wave function had been well optimized, but the quadratic correlations were included without any additional optimization. We included a simple optimization factor in the front of the independent pair correlations for ^4He and it is clear that additional optimization is needed to minimize the energy as can be seen in figure 2. The scaling of the calculations with independent pair and quadratic correlations in relation to the original linear correlations is given in Fig. 3. The scaling factors were calculated by comparing the average times it took to complete one block of calculations to the average times it took for the linear correlations.

To calculate the scaling the average time to complete one block of calculations was used.

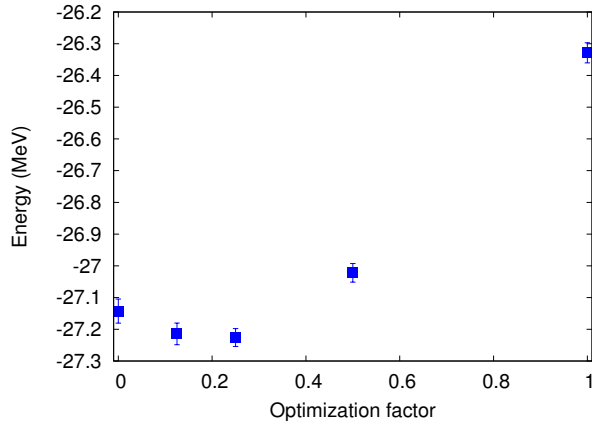


Figure 2: Energy for ^4He as a function of the quadratic correlation optimization parameter, calculated with independent pair correlations.

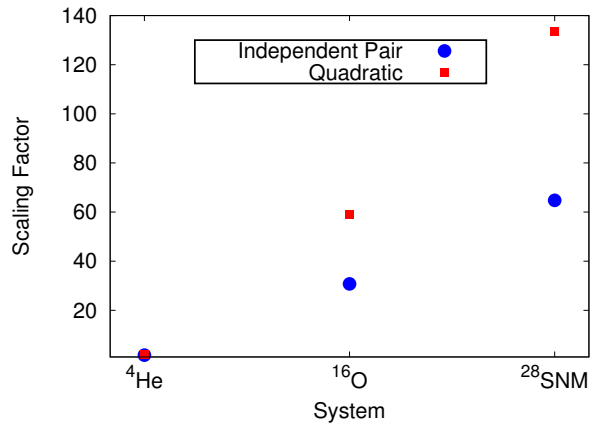


Figure 3: Scaling factors for ^4He , ^{16}O , and symmetric nuclear matter as calculated with the average time to complete a block of calculations. The factor is a ratio of the time to calculate the independent pair calculations compared to the time to calculate with the linear correlations. The factors are 1.73, 30.74 and 64.77 respectively for independent pair correlations, and 2.00, 58.83 and 133.59 for quadratic correlations..

5 Conclusion and Outlook

As mentioned before, one of the most important parts of the calculation is to have a good estimate for the trial wave function that is possible and inexpensive to calculate. So far we have implemented and tested a method for improving the trial wave function used in AFDMC calculation of nuclei and nuclear matter. We have done this by including independent pair and the full quadratic terms in the correlation operator which currently only has linear terms. The addition of these optimized terms has caused the energy of ^4He , ^{16}O and SNM to decrease.

Another way to improve the trial wave function is to include more terms in the expansion of the product correlation operator in Eq. 39. As we have learned from the independent pair

expansion that we implemented, this would get computationally intractable as the number of particles gets large. Another alternative is to rewrite the correlation operator in terms of a Hubbard-Stratanovich transformation as is done with the spin-isospin dependent part of the propagator in Sec. 2.5. Future work will be done to handle the correlation operators in this way. We will also be searching for additional ways to improve the trial wave function.

With an improved trial wave function we will be using AFDMC to investigate some interesting aspects of nuclear physics and nuclear astrophysics. For example, we will be investigating the formation of deuteron and alpha particle clusters at various densities in mostly neutron matter. Many types of clustering in physics deal with two particles at a time. Alpha particles are thus a special case of four fermion clustering due to the two additional isospin degrees of freedom in addition to the two spin states for spin 1/2 particles. Work has been done to show the light clustering ($A \leq 4$) and condensation of particles in nuclear systems, [24–26] including neutron stars [27–29]. We plan to show that the AFDMC method, with an improved nuclear wave function can be used to study properties of light clustering in nuclear systems as well. One way we will be doing this will be to do AFDMC calculation with 14 neutrons in a periodic box with the addition of 2 protons at a variety of densities to observe the formation of an alpha particle in neutron matter. Once these clusters are observed with AFDMC the density can be varied to determine the density at which the clusters dissolve as in Ref. [28]. This work will be especially applicable to the study of alpha formation in neutron stars.

In conclusion, we have done AFDMC calculations to calculate the energy of ^4He and ^{16}O as well as the energy per particle of SNM. We have done these calculations with both linear correlation terms, linear plus independent pair correlations and linear plus all of the quadratic correlations in the trial wave function. In order to maintain the cluster decomposability of the trial wave function, which is lost with either the linear or independent pair correlations, we will be using the Hubbard-Stratanovich transformation to sample the exponential spin-isospin dependent correlations. This is analogous to the sampling of spin-isospin states in the propagator of AFDMC. We will also be looking for additional ways to improve the trial wave function. We will then be applying these calculations to other interesting nuclear systems such as the clustering of alpha particles in neutron matter.

References

- [1] J. M. Lattimer and M. Prakash. Neutron star structure and the equation of state. *Astrophys. J.*, 550:426, 2001.
- [2] J. M. Lattimer and M. Prakash. The physics of neutron stars. *Science*, 304:536, 2004.
- [3] J. Rikowska Stone, J. C. Miller, R. Koncewicz, P. D. Stevenson, and M. R. Strayer. Nuclear matter and neutron-star properties calculated with the Skyrme interaction. *Phys. Rev. C*, 68, 2003.
- [4] F. Douchin and P. Haensel. A unified equation of state of dense matter and neutron star structure. *Astron. Astrophys.*, 380:151, 2001.
- [5] Henning Heiselberg and Vijay Pandharipande. Recent progresses in neutron star theory. *Annu. Rev. Nucl. Part. Sci.*, 50:481, 2000.
- [6] H. Yukawa. On the interaction of elementary particles. i. *Proc. Phys. Math. Soc. Japan.*, 17:48, 1935.
- [7] C. M. G. Lattes, H. Muirhead, G. P. S. Occhialini, and C. F. Powell. Processes involving charged mesons. *Nature*, 159:694–697, 1947.
- [8] Leonard S. Kisslinger and Debasish Das. Review of QCD, quark-gluon plasma, heavy quark hybrids, and heavy quark state production in p-p and A-A collisions. *Int. J. Mod. Phys. A*, 31, 2016.
- [9] Martin J. Savage. Nuclear physics. *Proc. Sci.*, 2016.
- [10] Petr Navrátil, Sofia Quaglioni, Ionel Stetcu, and Bruce R Barrett. Recent developments in no-core shell-model calculations. *Journal of Physics G: Nuclear and Particle Physics*, 36(8):083101, 2009.
- [11] Bruce R. Barrett, Petr Navrátil, and James P. Vary. *Ab initio* no core shell model. *Prog. Part. Nucl. Phys.*, 69:131–181, 2013.
- [12] G Hagen, T Papenbrock, M Hjorth-Jensen, and D J Dean. Coupled-cluster computations of atomic nuclei. *Rep. Prog. Phys.*, 77(9):096302, 2014.
- [13] W.H. Dickhoff and C. Barbieri. Self-consistent Green’s function method for nuclei and nuclear matter. *Prog. Part. Nucl. Phys.*, 52(2):377 – 496, 2004.
- [14] V. Somà, A. Cipollone, C. Barbieri, P. Navrátil, and T. Duguet. Chiral two- and three-nucleon forces along medium-mass isotope chains. *Phys. Rev. C*, 89:061301, Jun 2014.
- [15] H. Hergert, S.K. Bogner, T.D. Morris, A. Schwenk, and K. Tsukiyama. The in-medium similarity renormalization group: A novel *ab initio* method for nuclei. *Phys. Rep.*, 621:165–222, 2016. Memorial Volume in Honor of Gerald E. Brown.

- [16] J. Carlson, S. Gandolfi, F. Pederiva, Steven C. Pieper, R. Schiavilla, K.E. Schmidt, and R.B. Wiringa. Quantum Monte Carlo methods for nuclear physics. *Rev. Mod. Phys.*, 87:1067, 2015.
- [17] J. E. Lynn and K. E. Schmidt. Real-space imaginary-time propagators for non-local nucleon-nucleon potentials. *Phys. Rev. C*, 86:014324, Jul 2012.
- [18] J. C. Slater. A simplification of the Hartree-Fock method. *Phys. Rev.*, 81:385, 1951.
- [19] Robert Jastrow. Many-body problem with strong forces. *Phys. Rev.*, 98:1479, 1955.
- [20] M. H. Kalos. Monte Carlo calculations of the ground state of three- and four-body nuclei. *Phys. Rev.*, 128:1791, 1962.
- [21] K. E. Schmidt and S. Fantoni. A quantum Monte Carlo method for nucleon systems. *Phys. Lett. B*, 446:99–103, 1999.
- [22] W. M. C. Foulkes, L. Mitas, R. J. Needs, and G. Rajagopal. Quantum Monte Carlo simulations of solids. *Rev. Mod. Phys.*, 73:33–83, 2001.
- [23] R.B. Wiringa, R.A. Smith, and T.L. Ainsworth. Nucleon-nucleon potentials with and without $\Delta(1232)$ degrees of freedom. *Phys. Rev. C*, 29:1207, 1984.
- [24] P. Schuck, Y. Funaki, H. Horiuchi, G. Röpke, A. Tohsaki, and T. Yamada. α -particle condensation in nuclear systems. *Nucl. Phys. A*, 788:293c–300c, 2007.
- [25] P. Schuck, Y. Funaki, H. Horiuchi, G. Röpke, A. Tohsaki, and T. Yamada. Alpha-particle condensation in nuclear systems. *J. Phys.: Conf. Ser.*, 413:012009, 2013.
- [26] P. Schuck. Alpha-particle condensation in nuclear systems: present status and perspectives. *J. Phys.: Conf. Ser.*, 436:012065, 2013.
- [27] S. S. Avancini, C. C. Barros, D. P. Menezes, and C. Providência. α particles and the “pasta” phase in nuclear matter. *Phys. Rev. C*, 82:025808, Aug 2010.
- [28] S.S. Avancini, C.C. Barros Jr., L. Brito, S. Chiacchiera, D.P. Menezes, and C. Providência. Light clusters in nuclear matter and the “pasta” phase. *Phys. Rev. C*, 85:035806–1, 2012.
- [29] Ad.R. Raduta, F. Aymard, and F. Gulminelli. Clusterized nuclear matter in the (proto-)neutron star crust and the symmetry energy. *Eur. Phys. J. A*, 50:24, 2014.